Online Optimization and Control for Renewable Hybrid Power Plants

Claudiu Ionita, Alin George Raducu, Nikolaos Styliaras, Jonas Funkquist
Research and Development
Vattenfall AB
alingeorge.raducu@vattenfall.com

Abstract— **This paper presents a proposal for an optimization algorithm that maximizes the revenue of hybrid power plants (HPP), consisting of wind power plants, solar power plants and battery energy storage systems (BATT) that are connected in the same Point of Connection (POC). An online optimization, which has the goal to maximize the revenue, based on inputs such as plants operating costs, subsidy levels, market spot price and possible powers is developed. The optimization problem is solved by a linear programming solver. A set of constraints is introduced to ensure power limitation in the POC in case of overproduction and to ensure power availability for FCR delivery. Furthermore, an option is implemented to choose a prioritization of the service to be delivered, i.e. the power production setpoint or the FCR setpoint.**

Keywords - Control and Optimization of renewable energy sources, Hybrid power plant control and optimization, Hybrid power plant integration, Battery energy storage system.

I. Introduction

Climate change is an environmental problem that is very different from the more traditional areas of pollution, such as water, waste or air quality. Moreover climate change is a truly global environmental problem, as it does not matter where greenhouse gases are emitted – they have the same impact [1]. Thus, during the last decades, penetration rates of renewable energy sources (RES) generation have steadily increased due to environmental concerns and positive market stances [2] and this trend is expected to continue motivated by international regulations as well [1][3]. In fact, some countries already present high shares of RES generation in their power systems, e.g., 40.7% of the Danish electricity consumption was covered by wind power in 2018 [4].

Utility companies have, over the last years, investigated different solutions to decrease the levelized cost of energy and to increase the full load hours for existing or new wind farms (WF) assets. In general the full load hours oscillates around 35% and 45% for onshore and offshore, respectively [5]. Briefly, if additional generation units are added to the system, the under-utilization of the grid will be reduced. Different investor or sites owners are considering collocating different generation units (such as solar plants) in order to increase the production rate and/or complement it with a battery energy storage systems gaining flexibility towards grid codes compliance and ancillary services provision. Such a plant combining these three elements is referred to in this paper as a hybrid power plant (HPP) based on the benchmark model presented in previous work [6] [7]. Subsequently a HPP will be capable of providing increased power generation, power smoothing, production loss minimization and sudden power injections to help in the frequency regulation.

To enable and support all these functionalities mentioned above a new component will be required to be developed such as Hybrid Power Plant Controller (HPPC). A proof of concept of such hybrid power plant controller was developed first in a simulation environment and presented in previous work [6] [7] with the aim to be deployed in a future HPP. It concerns a completely new hybrid power plant composed by a Wind Farm interconnected in the same Point of Connection (POC) with a Solar Farm (SF) and Battery System that Vattenfall will develop and start to operate during 2020. This component will aim to real-time steer and optimize the active/reactive power generation as a function of different constraints such as: the demand requested in the POC, capacity of the main grid connection point or ancillary services provision. Moreover, different curtailment strategies will be developed and implemented as well. The curtailment of each component has different priorities and is performed through an optimization and dispatch function.

In the last years scientific publications regarding optimization-based control are published in the literature, but they mostly concern offline optimization [8] [9] [10] [11]. Some work has also been done within control of hybrid wind-solar-battery plants but they deal with control based on given weather and load conditions within a specific period [12] [13]. A real-time control algorithm is presented in [14], but the purpose there is to reduce the fluctuations in the output power at the connection point, utilizing the battery. Basic questions regarding the integration of new units to existing sites have not been addressed often.

II. Architectural Design

An architectural diagram of the entire system is shown in Fig. 1. The overall system is divided into two main parts as shown in the diagram: the Market System and the HPPC. The Market System consists of two main components Trading and

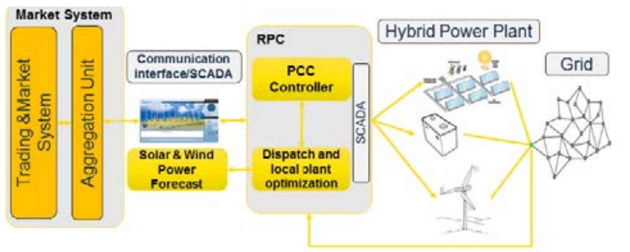

Figure 1. HPPC architectural diagram.

Market system and Aggregation Unit while the HPPC will contain a POC controller and a local dispatch and optimization and function. These two main components will be linked through a standard SCADA communication interface. This article will focus on describing the development of the local dispatch and optimization function.

III. Optimization

The optimization proposed for HPP has the aim of assuring the highest possible revenue, while ensuring that grid-related constraints are not violated, e.g. power limitation in the POC. It is assumed that all the plants are certified to deliver frequency containment reserve (FCR) which is also the main functionality of the battery.

Assuming that the HPP is treated as a single production unit and that the production setpoint and FCR setpoint must be tracked in the POC, the optimization must dispatch individual production and FCR setpoints to the plants units. The dispatch is based on power availability, operating costs, subsidy levels, penalty for setpoint error (imbalance cost), etc. A diagram of the suggested optimization is presented in Fig. 2.

A. Optimization Variables

A list of all the variables and parameters used in the optimization is presented in Table 1. The solution of the optimization consists of the production setpoints and the amount of FCR that each plant has to deliver, e.g. P^{WF}_{dmd}, $P^{WF}_{FCR,+}$ and $P^{WF}_{FCR,-}$. The decision variables of the optimization problem are:

$$x = [\, P^{WF}_{dmd};\ P^{SF}_{dmd};\ P^{WF}_{FCR,+};\ P^{WF}_{FCR,-};\ P^{SF}_{FCR,+};\ P^{SF}_{FCR,-};\ P^{BATT}_{FCR,+};\ P^{BATT}_{FCR,-};\ P^{POC}_{spt(err)};\ P^{POC}_{FCR+(err)};\ P^{POC}_{FCR-(err)}] \quad (1)$$

Notice the variables $P^{POC}_{spt(err)}$, $P^{POC}_{FCR+(err)}$ and $P^{POC}_{FCR-(err)}$ which are needed to select the service that should be prioritized if there is not sufficient possible power.

B. Cost Function

The purpose of the optimization problem is to maximize the revenue. The variables that influence the solution are the

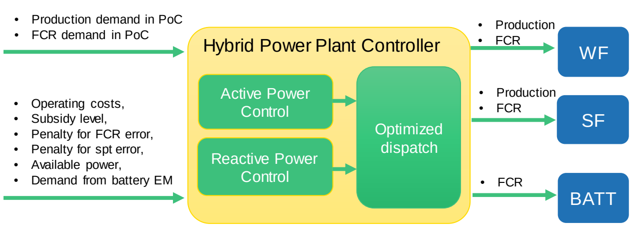

Figure 1. Figure 2: Inputs, outputs and main functions of the HPPC.

Parameters	Description	Unit
P^{POC}_{rated}	Rated power in the Point of Common Coupling	MW
$P^{\dots}_{poss}$	Possible power production	MW
$P^{\dots,pq}_{FCR,+}$	Prequalified power for positive FCR provision	MW
$P^{\dots,pq}_{FCR,-}$	Prequalified power for negative FCR provision	MW
r	Revenue for providing a service or subsidy	€/MW
c	Cost of operating a plant or penalty for not providing a specific service	€/MW
$P^{\dots}_{dmd}$	Power production demand from a plant	MW
$P^{\dots}_{FCR,+}$	Positive FCR demand from a plant	MW
$P^{\dots}_{FCR,-}$	Negative FCR demand from a plant	MW
$P^{\dots,pq}_{FCR}$	Prequalified FCR power	MW
P^{BATT}_{offset}	Power setpoint offset demanded by the battery's energy management system	MW
$P^{POC}_{spt(err)}$	Production imbalance	MW
$P^{POC}_{FCR(err)}$	Positive FCR or negative FCR imbalance	MW

Table 1. Nomenclature used in this paper. The … is substituted with WF, SF, and BATT representing wind farm, solar farm and battery system, repectively.

spot price, the subsidy levels, operational cost, penalty for not fulfilling the FCR and penalty for not delivering the agreed production (imbalance cost). The cost function is a linear expression implemented as:

$$f(x) = P^{WF}_{dmd}\cdot(r_{spot} + r^{WF}_{sub} - c^{WF}_{op}) + P^{SF}_{dmd}\cdot(r_{spot} + r^{SF}_{sub} - c^{SF}_{op}) - P^{POC}_{spt(err)}\cdot c^{POC}_{spt(err)} - P^{POC}_{FCR+(err)}\cdot c^{POC}_{FCR+(err)} - P^{POC}_{FCR-(err)}\cdot c^{POC}_{FCR-(err)} \quad (2)$$

C. Lower and Upper boundaries

The lower and upper boundaries are implemented to ensure that the physical capabilities of the optimization variables, such that the possible power and the prequalified FCR power are not exceeded:

$$0 \le P^{WF}_{dmd} \le P^{WF}_{poss} \quad (3)$$
$$0 \le P^{SF}_{dmd} \le P^{SF}_{poss} \quad (4)$$
$$0 \le P^{WF}_{FCR,+} \le P^{WF,pq}_{FCR,+} \quad (5)$$
$$0 \le P^{WF}_{FCR,-} \le P^{WF,pq}_{FCR,-} \quad (6)$$
$$0 \le P^{SF}_{FCR,+} \le P^{SF,pq}_{FCR,+} \quad (7)$$
$$0 \le P^{SF}_{FCR,-} \le P^{SF,pq}_{FCR,-} \quad (8)$$
$$0 \le P^{BATT}_{FCR,+} \le P^{BATT,pq}_{FCR,+} \quad (9)$$
$$0 \le P^{BATT}_{FCR,-} \le P^{BATT,pq}_{FCR,-} \quad (10)$$
$$0 \le P^{POC}_{spt(err)} \quad (11)$$
$$0 \le P^{POC}_{FCR+(err)} \quad (12)$$
$$0 \le P^{POC}_{FCR-(err)} \quad (13)$$

D. Inequality constraints

The inequality constrains (14) and (15) ensure that the sum of the FCR demand and the production demand does not exceed the possible power. Contrary to the battery, the WF and SF need to have some production in order to deliver negative FCR, which is taken into account by the constraints

(16) and (17). Limitations related to the POC rating and incorporated in (18) and (19).

$$P^{WF}_{dmd} + P^{WF}_{FCR,+} \leq P^{WF}_{poss} \quad (14)$$
$$P^{SF}_{dmd} + P^{SF}_{FCR,+} \leq P^{SF}_{poss} \quad (15)$$
$$-P^{WF}_{dmd} + P^{WF}_{FCR,-} \leq 0 \quad (16)$$
$$-P^{SF}_{dmd} + P^{SF}_{FCR,-} \leq 0 \quad (17)$$
$$P^{WF}_{dmd} + P^{SF}_{spt} + P^{WF}_{FCR,+} + P^{SF}_{FCR,+} + P^{BATT}_{FCR,+} \leq P^{POC}_{rated} - P^{BATT}_{offset} \quad (18)$$
$$-P^{WF}_{dmd} - P^{SF}_{dmd} + P^{WF}_{FCR,-} + P^{SF}_{FCR,-} + P^{BATT}_{FCR,-} \leq P^{BATT,pq}_{FCR,-} \quad (19)$$

E. *Equality constraints*

A set of equality constraints is also needed to provide a calculation of the FCR and power production setpoint errors in the POC. For the case where symmetrical FCR behavior is desired (23) is also added.

$$P^{WF}_{dmd} + P^{SF}_{dmd} + P^{POC}_{spt(err)} = P^{POC}_{spt} - P^{BATT}_{spt} \quad (20)$$
$$P^{WF}_{FCR+} + P^{SF}_{FCR+} + P^{BATT}_{FCR+} + P^{POC}_{FCR+(err)} = P^{POC}_{FCR+} \quad (21)$$
$$P^{WF}_{FCR-} + P^{SF}_{FCR-} + P^{BATT}_{FCR-} + P^{POC}_{FCR-(err)} = P^{POC}_{FCR-} \quad (22)$$
$$P_{FCR+} = P_{FCR-} \quad (23)$$

IV. Test Cases and Simulation Results

A series of test cases has been developed and simulated in order to verify that the optimization behaves as intended. A plant with the characteristics presented in Table 2 is used. The model of the WF, SF and BESS used for dynamic simulations has been presented in [6].

Since FCR is considered a system critical service, it is assumed that the penalty for not delivering the service is very high, in a real application not delivering FCR can lead to quarantine or losing the right to participate in the FCR market. Here, however, we introduce a penalty factor (e.g. $c^{POC}_{FCR+(err)}$ in (2)) which is chosen high in order to prioritize FCR over power production.

Due to the complexity of the system a large number of scenarios can be created, but only the most relevant test cases will be presented here.

A. *Test Case 1: Step changes in production setpoint with fixed possible power*

With this test case it is desired to verify that the plant is capable of following a specific power production setpoint when no FCR is demanded. This is achieved by performing step changes in the power production setpoint, assuming constant possible power from the WF and SF. For this scenario it is assumed that the WF should be curtailed first, due to higher revenue streams of the SF, based on operating costs. This might however change if a load mitigation strategy is chosen instead, where the SF should be curtailed first in case of overproduction, since the mechanical stress on the components in the SF is usually less compared to the WF.

The results of the simulation are presented in Fig. 3. The functionality of power limitation works as intended, as it can be seen in Fig. 3a. In this case, this is achieved by curtailing the WF as seen in Fig. 3e.

Component	Size	Unit
POC limit	150	MW
WF rating	122.4	MW
SF rating	40	MW
BATT rating	12	MW/MWh
r_{spot}	50	€/MWh
r^{WF}_{sub}	17	€/MWh
c^{WF}_{op}	7	€/MW
r^{SF}_{sub}	17	€/MWh
c^{SF}_{op}	5	€/MW

Table 2. HPP component rating and cost/revenue levels used in the TC.

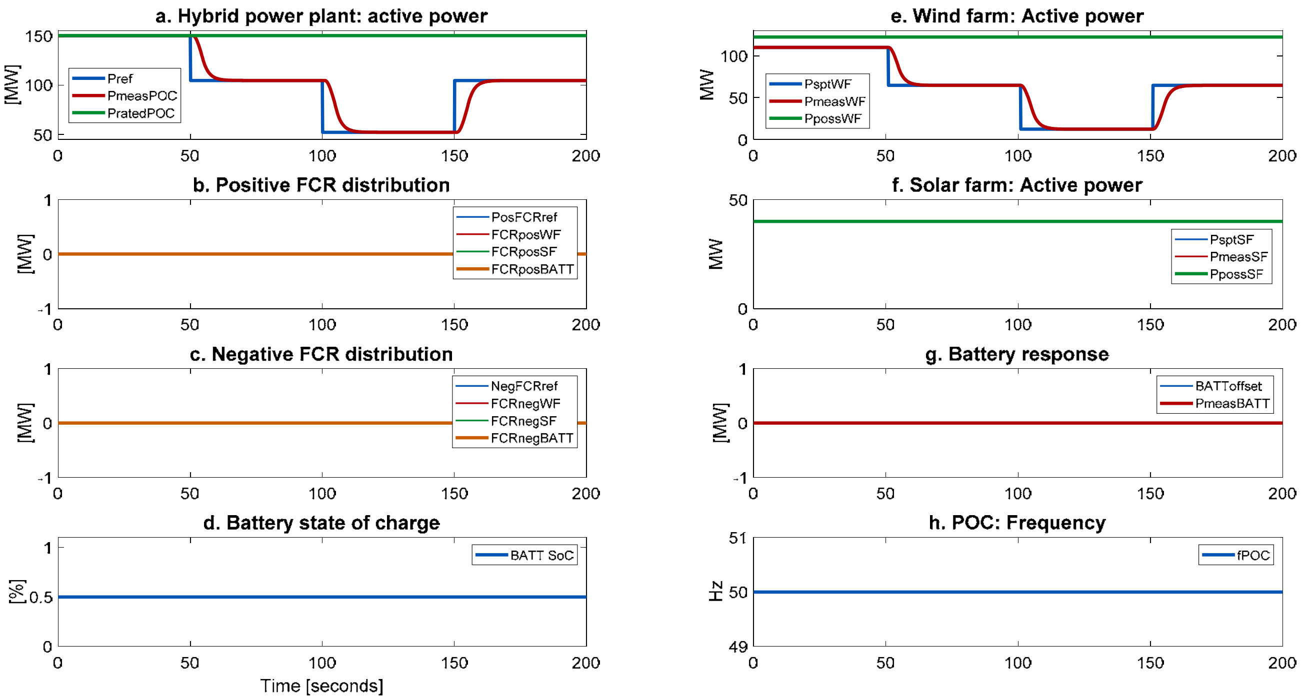

Figure 3. Test Case 1: HPP response to power production setpoints and no FCR demand.

B. *Test Case 2: FCR demand setpoint with fixed possible power*

In this test case, it is desired to observe that the HPPC is able to distribute correct FCR setpoints to the individual assets and to verify that the plants respond properly to frequency deviations. Fig. 4h shows the frequency variation and Fig. 4b and 4c show, respectively, the FCR demand distribution. The responses of the different plants are shown in Fig. 4e-g. Since, the main functionality of the battery is FCR, it will always provide the service as the first option. In the case of positive FCR, the service is also provided by the WF, while for the negative FCR, the optimal way to provide FCR is with the SF in addition to the battery.

C. *Test Case 3: Step changes in production setpoint and FCR demand with varying possible power*

With this test case it is desired to investigate the behavior of the HPP for a more realistic scenario where the possible power of the WF and SF is fluctuating. A step change in power production demand has also been introduced at t=6000 s to verify that the plant is able to follow the setpoint (see Fig. 5a). In Fig. 5e, it can be seen how the WF is curtailed, while maintaining the required spinning reserve to be able to provide positive FCR. In Fig. 5c between t = 0s and t = 500 s, it can be seen (as small fluctuations) how the WF and SF complement each other to deliver the required negative FCR.

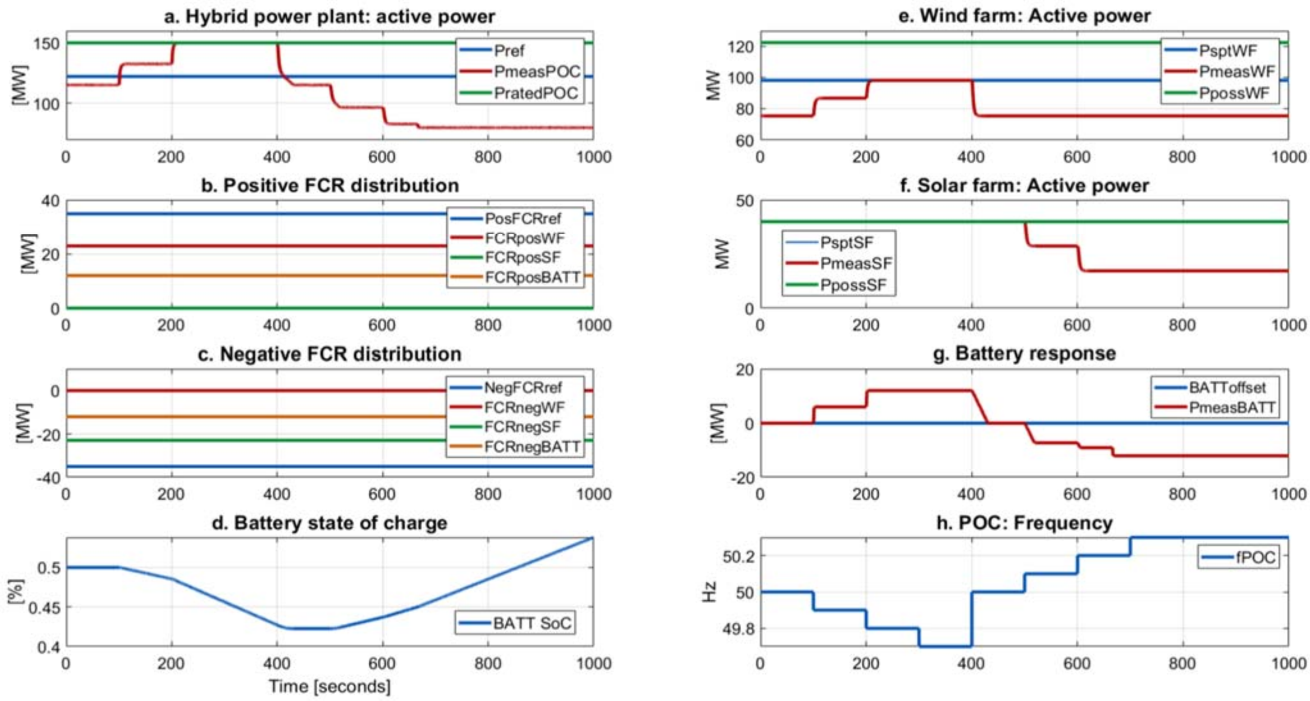

Figure 4. Test Case 2: HPP response to FCR demand and fixed possible power.

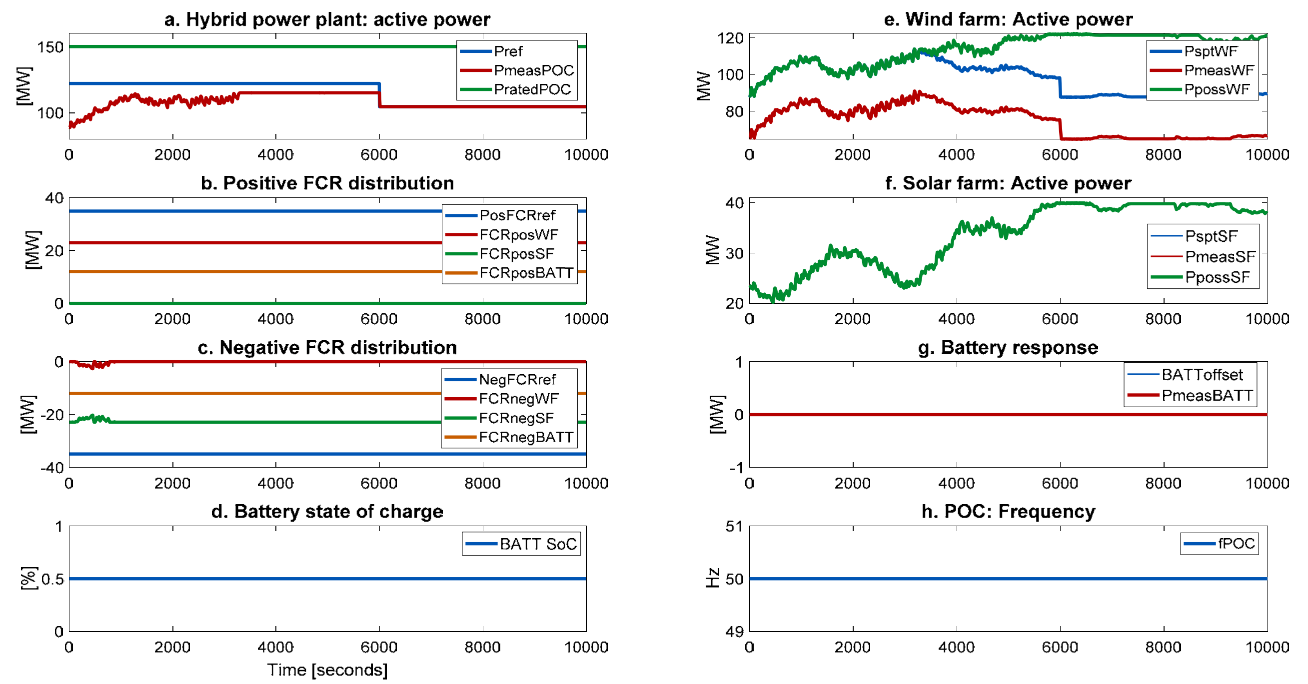

Figure 5. Test Case 3: HPP response to power production and FCR demand with varying possible power.

D. Test Case 4: FCR demand with varying possible power and frequency

This case is based on test case 3 with the main difference that the frequency is also varied. At t=250 step changes in the frequency are applied to simulate an event of underfrequency, see Fig 6h. The battery responds by injecting power to the grid (Fig. 6g). It can also be noticed that in some cases a power ramp is applied to the battery. This is due to the fact that in Germany and Netherlands some degrees of freedom can be used to manage the battery energy level free of charge [15].

Regarding the WF, until t=250 s, it curtails the requested power and at t=300 s when the frequency deviation is 200 mHz it injects all the power that it has available for the positive FCR (Fig. 6e). At t=500 s, the frequency returns to 50 Hz and the WF restores the requested spinning reserve.

The SF is not providing any positive FCR, since it can be covered by the WF. However the SF is assigned to deliver negative FCR. At t=1000 s a frequency increase is simulated and the SF curtails its power production to deliver negative FCR (Fig. 6f). As in test case 2, the battery provides both positive and negative FCR (Fig 6g).

E. Test Case 5: WF subsidy higher than SF subsidy

The impact of having higher subsidy for the WF compared to the SF is investigated in this test case. This should lead to a prioritization of power production from WF and delivery of positive FCR from the SF as the first option. It is therefore assumed that the WF subsidy, r_{sub}^{WF} has a value of 25 €/MWh while the subsidy for the SF is kept at 17 €/MWh. The results are illustrated in Fig. 7. From t=0 s to t=200 s, The SF is curtailed in order to have spinning reserve (Fig 7f) and at t=200 s when the frequency starts to deviate from 50 Hz, the SF injects power into the grid to compensate for the frequency deviation. At t=500 s, the frequency returns to 50 Hz and the SF is completely curtailed. The WF is also slightly curtailed in order to compensate for the missing capability of the SF to deliver the entire FCR (Fig. 7e). At t= 1000 s an event of over-frequency occurs and the negative FCR is mainly provided by the WF, since the SF does not have any production at that point. This test case is a good example of how the WF and SF can complement each other and enable provision of a higher volume of FCR from a HPP than would be possible if each plant are participating individually.

V. Conclusion and Discussion

This paper has presented an optimization controller that has the role of maximizing the revenue for a hybrid power plant, i.e. a plant composed of a wind farm, a solar farm and a battery. The role of the optimization is also to ensure a power limitation in the POC in case of overproduction, while ensuring an optimal distribution of FCR and power production setpoints that are sent to the individual assets. With the simulated test cases, it was possible to show that the optimization behaves as intended. Even though the optimization should maximize the revenue, the analysis presented here is focused on the technical aspects of the solution and not so much on the actual financial benefits.

In order to evaluate the true potential of the optimization on a yearly basis, this should be compared to a control solution where the distribution of setpoints is prespecified. Furthermore, in the proposed solution, it was assumed that the WF controller and SF controller can accurately calculate the possible power. In a field implementation, a function should also be implemented to correct for the likely possible power estimation errors.

Hybrid power plants containing wind farms, solar farms and batteries with installed overcapacity have many advantages and the potential to reduce the levelized energy cost, but it also comes with new challenges compared to having individual assets, as proven in this study. This emphasizes the need of further research in the topic to achieve the best operation of such a plant.

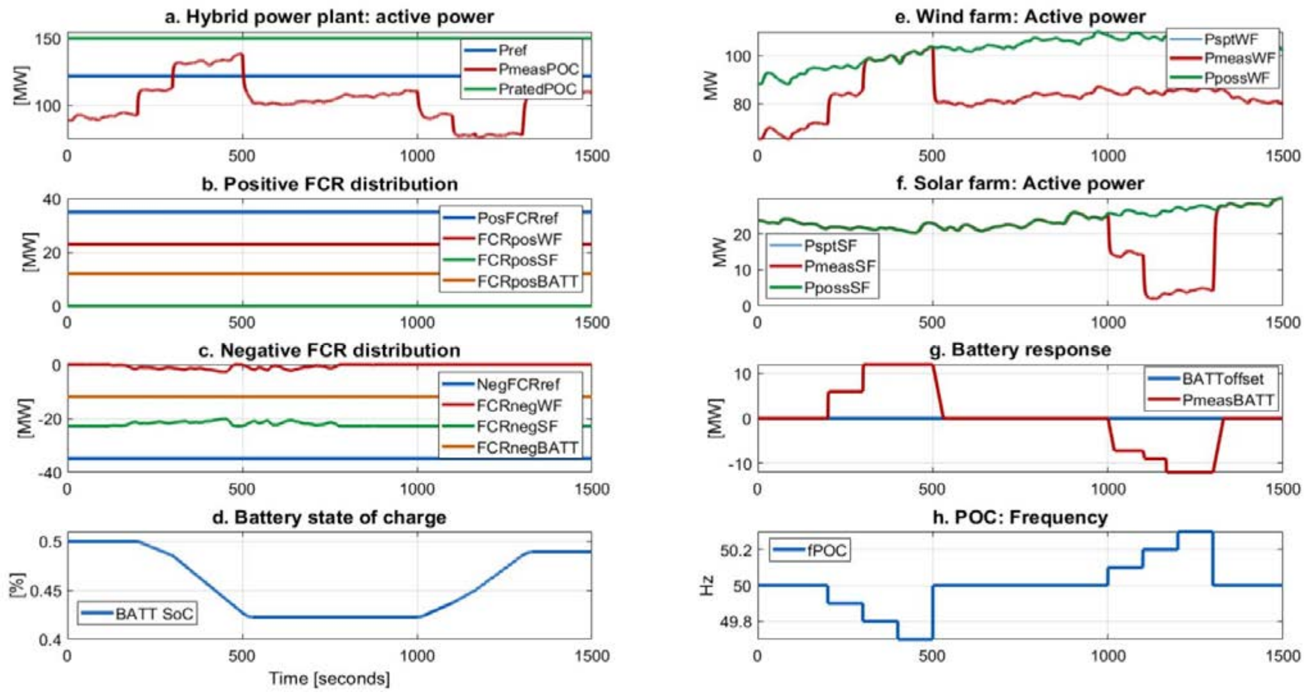

Figure 6. Test Case 4: FCR demand with varying possible power and frequency.

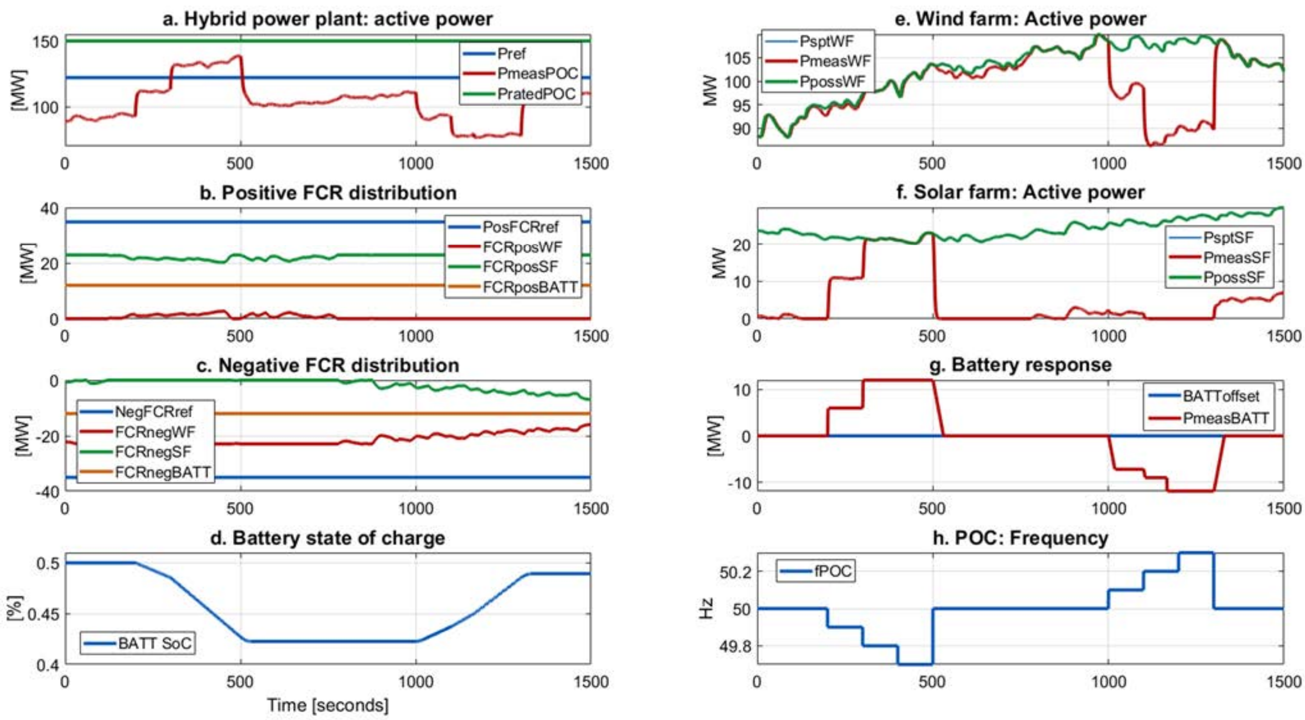

Figure 7. Test Case 5: FCR demand with varying possible power and frequency. WF subsidy is increased to 25 €/MWh while the subsidy for SF is kept at 17 €/MWh.

REFERENCES

[1] Delbeke, J.; Vis, P. EU Climate Policy Explained. Available online:https://ec.europa.eu/clima/sites/clima/files/eu_climate_policy_explained_en.pdf

[2] Ren21 Renewables 2017 Global Status Report. Available online:http://www.ren21.net/wp-content/uploads/2017/06/17-8399_GSR_2017_Full_Report_0621_Opt.pdf

[3] Plessmann, G.; Blechinger, P. How to meet EU GHG emission reduction targets? A model based decarbonization pathway for Europe's electricity supply system until 2050. Energy Strategy Rev. **2017**, 15, 19–32.

[4] Energinet Environmental Report 2018. Available online: https://en.energinet.dk/About-our-reports/Reports/Annual-report-2018

[5] Chabot, B. Onshore and OffshoreWind Power Capacity Factors: How Much They Differ Now and in the Future. 2013.Available online: https://www.erneuerbareenergien.de/files/smfiledata/3/1/7/2/7/1/

[6] A.G.Raducu, N. Styliaras, J. Funkquist and C.Ionita, "Design and Implementation of a Hybrid Power Plant Controller", 3rd International Hybrid Power Systems Workshop, Tenerife, Spain, 2018

[7] C.Ionita, A.G.Raducu, N. Styliaras, J. Funkquist and, "Optimal provision of Frequency Containment Reserve with Hybrid Power Plants", Wind Inteegration Workshop Conference, Stockholm, 2018

[8] S. Li, F. Sun, H. He and Y. Chen, "Optimization for a grid-connected hybrid PV-wind-retired HEV battery microgrid system", Energy Procedia, Volume 105, 2017

[9] M. J. B. Fulzele and M. B. Daigavane, "Design and optimization of hybrid PV-Wind renewable energy system", Materials Today: Proceedings, Volume 5, Issue 1, Part 1, 2018

[10] N. V. Rozhentcova, P. V. Ganin and A. I. Rudakov, "Structural and computer optimization model of a solar-wind hybrid electrical system in the software environment Matlab-Simulink", 2017 International Conference on Industrial Engineering, Applications and Manufacturing (ICIEAM), St. Petersburg, 2017

[11] Um. Akram, M. Khalid and S. Shafiq, "An innovative hybrid wind-solar and battery-supercapacitor microgrid system – development and optimization", IEEE Access, vol. 5, 2017

[12] N. V. Rozhentcova, P. V. Ganin and A. I. Rudakov, "Structural and computer optimization model of a solar-wind hybrid electrical system in the software environment Matlab-Simulink", 2017 International Conference on Industrial Engineering, Applications and Manufacturing (ICIEAM), St. Petersburg, 2017

[13] Um. Akram, M. Khalid and S. Shafiq, "An innovative hybrid wind-solar and battery-upercapacitor microgrid system – development and optimization", IEEE Access, vol. 5, 2017

[14] C. Peng, J. Zou, Z. Zhang, L. Han and M. Liu, "An ultra-short-term pre-plan power curve based smoothing control approach for grid-connected wind-solar-battery hybrid power system", IFAC-PapersOnLine, Volume 50, Issue 1, 2017

[15] J.Fleer, P. Stenzel, "Impact analysis of different operation strategies for battery energy storage systems providing primary control reserve", Journal of Energy Storage 8 (2016) 320-338.